

Threshold Resummation for $W^\pm Z$ and ZZ Pair Production at the LHC

Yan Wang,¹ Chong Sheng Li,^{1,2,*} Ze Long Liu,¹ and Ding Yu Shao¹

¹*Department of Physics and State Key Laboratory of Nuclear Physics and Technology,
Peking University, Beijing 100871, China*

²*Center for High Energy Physics, Peking University, Beijing, 100871, China*

Abstract

We perform the threshold resummation for $W^\pm Z$ and ZZ pair production at the next-to-next-to-leading logarithmic accuracy in Soft-Collinear Effective Theory at the LHC. Our results show that the resummation effects increase the total cross sections by about 7% for ZZ production and 12% for $W^\pm Z$ production with $\sqrt{S} = 7, 8, 13$ and 14 TeV, respectively, and the scale uncertainties are significantly reduced. Besides, our numerical results are well consistent with experimental data reported by the ATLAS and CMS collaborations.

PACS numbers: 12.38.Bx, 14.70.-e, 14.70.Hp, 14.70.Fm

*Electronic address: csli@pku.edu.cn

I. INTRODUCTION

The gauge boson pair production plays an important role at the LHC, not only for testing the $SU(2) \times U(1)$ gauge structure of the Standard Model (SM), but also for understanding the background of the SM Higgs and the new physics signal. In particular, ZZ production is the irreducible background process to the SM Higgs boson signal. Besides, the WWZ tri-linear coupling, which can be used to search for heavy charged gauge boson, is constrained by the $W^\pm Z$ production. Deviations between the measured data and the SM predictions in the total or the differential cross sections, may suggest a new physics signals. Consequently, the study of the precise theoretical predictions for $W^\pm Z$ and ZZ production at the LHC are necessary.

Collaborations at the Tevatron and the LHC have reported experimental results for $W^\pm Z$ and ZZ productions, respectively. The measurements for the total and differential cross sections through the leptonic decay mode have been analyzed at the Tevatron [1–3]. Both ATLAS [4–9] and CMS [10–13] collaborations have also presented leptonic decay results at the LHC. Besides, $W^\pm Z$ and ZZ cross sections, where one Z boson decays to b-tagged jets, have been measured by CMS collaboration [14]. However, the data which are currently available from the LHC have large experimental uncertainties [15], so it is worth to make an accurate theoretical predictions beyond QCD NLO to figure out whether the discrepancies come from the theoretical errors or the new physics. The QCD NLO corrections for the production of $W^\pm Z$ and ZZ have been studied in Refs. [16–22]. The transverse momentum resummation for gauge boson pair productions have been calculated in Ref. [23]. In Ref. [24], $W^\pm Z$ production is calculated beyond NLO for high q_T region. However, Next-to-Next-to-Leading-Order (NNLO) are still in progress. Very recently, the NNLO corrections to the ZZ production are presented for the LHC [25–29]. However, in order to compare the total cross section and some kinetic distribution, such as invariant mass distributions, we still need to consider the effects of soft gluon emission near the threshold region. The soft gluon resummation and the approximate NNLO cross sections for W^+W^- pair production were calculated in Ref. [30], and we have repeated their resummation results as a cross check.

In this paper, we calculate the threshold resummation for $W^\pm Z$ and ZZ pair production at the Next-to-Next-Leading Logarithmic (NNLL) accuracy based on Soft-Collinear Effective Theory (SCET) [31–33]. The paper is organized as follows. In Sec. II, we describe the

formalism for threshold resummation in SCET briefly. In Sec. III, we present the numerical results and some discussion. Then Sec. IV is a brief conclusion.

II. FACTORIZATION AND RESUMMATION

In this section, we briefly review the threshold resummation in SCET formalism in this paper, following the Ref [34]. We consider the process

$$N_1(p_1) + N_2(p_2) \rightarrow V(p_3) + Z(p_4) + X(p_x), \quad (1)$$

where $V(=W, Z)$ is a W or Z boson, and X denotes any hadronic final states. In the Born level, the gauge boson pair is mainly produced through $q\bar{q}'$ process:

$$q(p_1) + \bar{q}'(p_2) \rightarrow V(p_3) + Z(p_4), \quad (2)$$

where $p_i = z_i P_i$, $i = 1, 2$. We define the kinematic variables as follows

$$S = (P_1 + P_2)^2, \quad \hat{s} = (p_1 + p_2)^2, \quad \tau = M_{VZ}^2/S, \quad z = M_{VZ}^2/\hat{s}. \quad (3)$$

where M_{VZ} is the invariant mass of the gauge boson pair. During the derivation of factorization expression, the scale hierarchy is assumed in the threshold region:

$$\hat{s}, M_{VZ}^2 \gg \hat{s}(1-z)^2 \gg \Lambda_{\text{QCD}}^2, \quad (4)$$

where \hat{s}, M_{VZ}^2 are referred to as hard scales and $\hat{s}(1-z)^2$ is the soft scale. $\lambda = (1-z) \ll 1$ is the expansion parameter. In the threshold limit, i.e. $\lambda \rightarrow 0$, the cross section can be factorized as

$$\frac{d\sigma}{dM_{VZ}^2} = \frac{\sigma_0}{S} \sum_{q, \bar{q}'} \int \frac{dx_1}{x_1} \frac{dx_2}{x_2} f_q(x_1, \mu_f) f_{\bar{q}'}(x_2, \mu_f) \mathcal{H}_{VZ}(M_{VZ}, \mu_f) \mathcal{S}(\sqrt{s}(1-z), \mu_f), \quad (5)$$

where σ_0 is the tree level cross section and $\mathcal{S}(-\sqrt{s}(z-1), \mu_f)$ is the soft function, which given by the vacuum expectation values of soft Wilson loops, while $\mathcal{H}_{VZ}(M_{VZ}, \mu)$ is the hard function, and can be expanded in powers of α_s :

$$\mathcal{H}_{VZ} = \mathcal{H}_{VZ}^{(0)} + \frac{\alpha_s}{4\pi} \mathcal{H}_{VZ}^{(1)} + \dots. \quad (6)$$

Here $\mathcal{H}_{VZ}^{(n)}$ can be extracted by matching the perturbative QCD results onto the relevant SCET operator, and the corresponding complete expression can be found in Ref. [23].

The renormalization-group equation for the hard function can be written as

$$\frac{d}{d \ln \mu} \mathcal{H}_{VZ}(M_{VZ}, \mu) = 2 \left[\Gamma_{\text{cusp}}^F(\alpha_s) \ln \frac{-M_{VZ}^2}{\mu^2} + 2\gamma^q(\alpha_s) \right] \mathcal{H}_{VZ}(M_{VZ}, \mu), \quad (7)$$

There also exist large π^2 terms in the hard function arising from the negative arguments in the squared logarithmic terms, which can be resummed to all order if we choose the hard scale as $\mu_h^2 \sim -M_{VZ}^2$ and then evolve μ_h^2 from the time-like region to the space-like region. Meantime we need the strong coupling $\alpha_s(\mu^2)$ evaluated at time-like region, and the strong coupling at time-like region $\alpha_s(-\mu^2)$ is related to the running couplings at the space-like region $\alpha_s(\mu^2)$ at NLO by the equation [35]

$$\frac{\alpha_s(\mu^2)}{\alpha_s(-\mu^2)} = 1 - ia(\mu^2) + \frac{\alpha_s(\mu^2)}{4\pi} \left[\frac{\beta_1}{\beta_0} \ln[1 - ia(\mu^2)] \right] + \mathcal{O}(\alpha_s^2), \quad (8)$$

where $a(\mu^2) = \beta_0 \alpha_s(\mu^2)/4$.

The soft function $\mathcal{S}(s(1-z)^2, \mu)$ can be defined as [34]

$$\mathcal{S}(s(1-z)^2, \mu) = \sqrt{s} W(s(1-z)^2, \mu), \quad (9)$$

where the $W(s(1-z)^2, \mu)$ function obeys the form:

$$\omega W(\omega^2, \mu_f) = \exp(-4S(\mu_s, \mu_f) + 2a_{\gamma W}(\mu_s, \mu_f)) \tilde{s}(\partial_\eta, \mu_s) \left(\frac{\omega^2}{\mu_s^2} \right)^\eta \frac{e^{-2\gamma\eta}}{\Gamma(2\eta)}, \quad (10)$$

where μ_s is the soft scale, $\eta = 2a_\Gamma(\mu_s, \mu_f)$, and the Sudakov exponent S and the exponents a_Γ are defined as

$$S(\nu, \mu) = - \int_{\alpha_s(\nu)}^{\alpha_s(\mu)} d\alpha \frac{\Gamma_{\text{cusp}}^F(\alpha)}{\beta(\alpha)} \int_{\alpha_s(\nu)}^{\alpha} \frac{d\alpha'}{\beta(\alpha')}, \quad (11)$$

$$a_\Gamma(\nu, \mu) = - \int_{\alpha_s(\nu)}^{\alpha_s(\mu)} d\alpha \frac{\Gamma_{\text{cusp}}^F(\alpha)}{\beta(\alpha)}. \quad (12)$$

The soft Wilson loop under the Laplace transformation is $\tilde{s}(L_s, \mu_s)$. Up to NLO, it can be expressed as

$$\tilde{s}(L_s, \mu_s) = 1 + \frac{C_F \alpha_s(\mu_s)}{4\pi} \left(2L_s^2 + \frac{\pi^2}{3} \right). \quad (13)$$

After combining the soft and hard function, the differential cross section can be factorized as

$$\frac{d\sigma}{dM_{VZ}^2} = \frac{\sigma_0}{S} \int_\tau^1 \frac{dz}{z} \mathcal{L}\left(\frac{\tau}{z}, \mu_f\right) \mathcal{H}_{VZ}(M_{VZ}, \mu_h) C(M_{VZ}, \mu_h, \mu_s, \mu_f), \quad (14)$$

where

$$\mathcal{L}(y, \mu_f) = \sum_{q, \bar{q}'} \int_y^1 \frac{dx}{x} [f_q(x, \mu_f) f_{\bar{q}'}(y/x, \mu_f)], \quad (15)$$

and $C(M_{VZ}, \mu_h, \mu_s, \mu_f)$ can be written as

$$C(M_{VZ}, \mu_h, \mu_s, \mu_f) = \exp[4S(\mu_h, \mu_s) - 2a_{\gamma^V}(\mu_h, \mu_s) + 4a_{\gamma^\phi}(\mu_s, \mu_f)] \left(\frac{M_{VZ}^2}{\mu_h^2} \right)^{-2a_\Gamma(\mu_s, \mu_h)} \\ \frac{(1-z)^{2\eta-1}}{z^\eta} \tilde{s} \left[\ln \left(\frac{(1-z)^2 M_{VZ}^2}{z \mu_s^2} \right) + \partial_{\eta, \mu_s} \right] \frac{e^{-2\gamma\eta}}{\Gamma(2\eta)}. \quad (16)$$

In addition to the singular terms, we should also use contributions from the non-singular terms, which can be obtained by matching resummed results to the full fixed order cross section. Finally, the Renormalization-Group improved prediction for the gauge boson pair production can be expressed as

$$\frac{d\sigma^{\text{NNLL+NLO}}}{dM_{VZ}^2} = \frac{d\sigma^{\text{NNLL}}}{dM_{VZ}^2} + \left(\frac{d\sigma^{\text{NLO}}}{dM_{VZ}^2} - \frac{d\sigma^{\text{NNLL}}}{dM_{VZ}^2} \right)_{\text{expanded to NLO}}. \quad (17)$$

III. NUMERICAL RESULTS

In this section, we present the numerical results for the threshold resummation effects on gauge boson pair production. We choose SM input parameters as following [36]:

$$m_W = 80.4 \text{ GeV}, \quad m_Z = 91.19 \text{ GeV}, \quad \alpha(m_Z) = 1/132.338. \quad (18)$$

Throughout the paper, we use MSTW2008nnlo PDFs and associated running QCD coupling constant for the resummation results. The factorization scale is set as the invariant mass M_{VZ} . The fixed-order QCD NLO corrections are calculated by MCFM [20] with MSTW2008nlo PDFs unless specified otherwise, where we consistently choose factorization and renormalization scales as M_{VZ} .

A. Scale setting and scale uncertainties

Before the numerical calculation, two additional scales, the hard scale μ_h and the soft scale μ_s , also need to be fixed. Generally, the hard scale should be fixed at $\mu_h \sim M_{VZ}$, where the hard Wilson coefficient have stable perturbative expansions. However, in order to include the π^2 enhancement effects, we choose $\mu_h^2 = -M_{VZ}^2$.

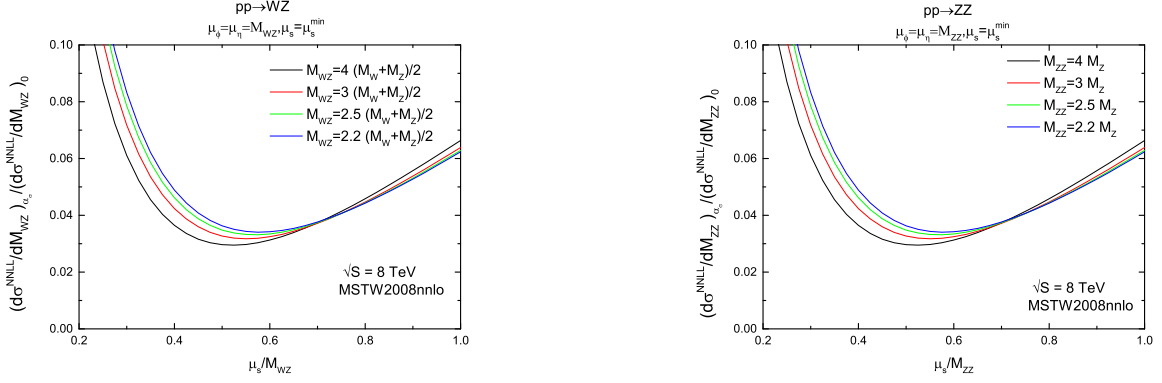


FIG. 1: The contribution of the NNLL resummed results arising from the one-loop corrections of the soft functions as a function of μ_s/M_{VZ} .

In Fig. 1, the dependence of the relative corrections of the soft functions at $\mathcal{O}(\alpha_s)$ on the soft scale μ_s are presented at the LHC with $\sqrt{S} = 8$ TeV. The requirement on μ_s is that the soft function should have a well-behaved perturbative stability. Thus, we determine μ_s by finding out where the corrections from the soft function is minimized. Because the soft function $\mathcal{S}(s(1-z)^2, \mu)$ is sensitive to the variable z and to the shape of the PDFs, we should integrate the soft function convoluting PDFs over z , and the integration results with different invariant mass are corresponding to the different lines in Fig. 1. As a result, μ_s is chosen at the minimum point of each line, which can be well parameterized in the form of

$$\mu_s = M_{VZ}(1 - \tau) (a + b\sqrt{\tau})^{-c}. \quad (19)$$

The situation with $\sqrt{S} = 14$ TeV is similar, and not shown here. Finally, the parameters are chosen as following:

$$\begin{aligned} \mu_{s,W^\pm Z}^{\min} &= M_{W^\pm Z} \frac{1 - \tau}{(3.004\sqrt{\tau} + 1.339)^{2.134}}, \\ \mu_{s,ZZ}^{\min} &= M_{ZZ} \frac{1 - \tau}{(3.013\sqrt{\tau} + 1.323)^{2.356}}. \end{aligned} \quad (20)$$

In Fig. 2, we show the scale dependence of the resummed cross sections on the hard scale and the soft scale with $\sqrt{S} = 14$ TeV. They turns out that the scale dependences are very tiny, less than 2%. In the plots, we also present the results after including π^2 effects, which decrease the dependence of the hard scale by about 50% comparing with the value without π^2 effects.

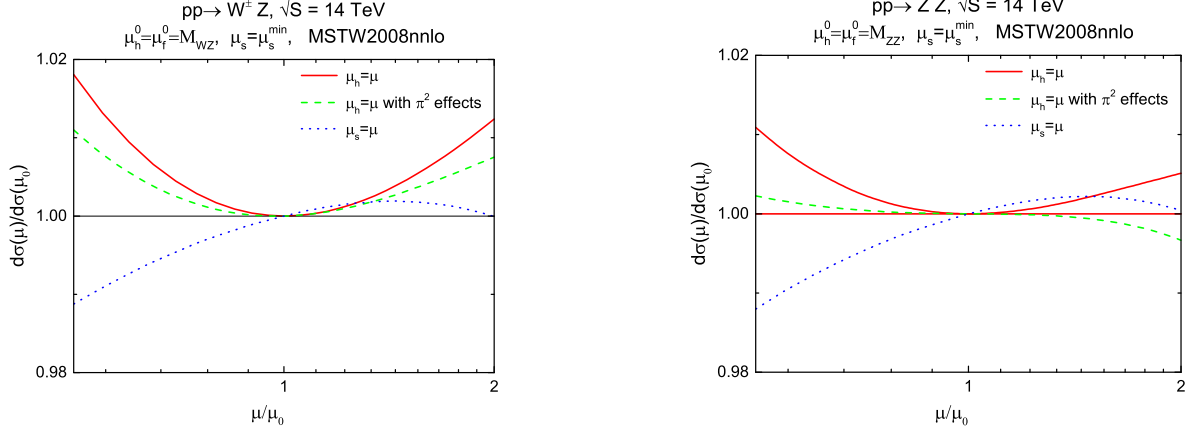


FIG. 2: Scale dependence of the resummed cross section on the hard scale, soft scale at NNLL level when $\sqrt{S} = 14$ TeV.

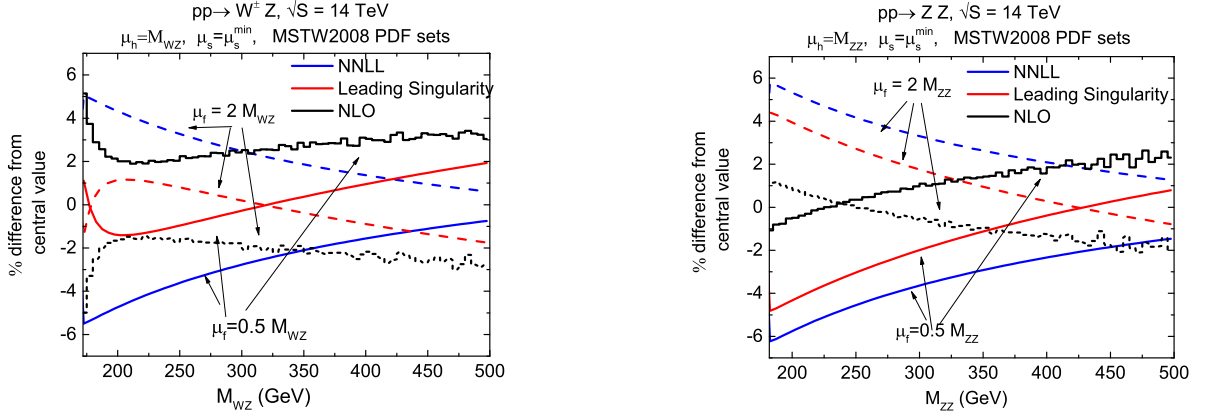


FIG. 3: Factorization scale dependence of the NNLL resummed part, the leading singularity part and the fixed-order part at $\sqrt{S} = 14$ TeV.

Fig. 3 and Fig. 4 show the factorization scale dependences on the invariant mass for $W^\pm Z$ and ZZ production. In Fig. 3, we compare the factorization scale dependence of the resummed part, the leading singularity part and the fixed-order part in Eq (17), where μ_f are changed from $M_{VZ}/2$ to $2M_{VZ}$. The dependence are defined as the ratio of their respective central value. We find that the scale dependence of the resummed part and the leading singularity part have the same tendency, while that of the NLO part is opposite to the resummed part, so that they cancel each other according to Eq. (17).

The full factorization scale dependences on the invariant mass are described in Fig. 4

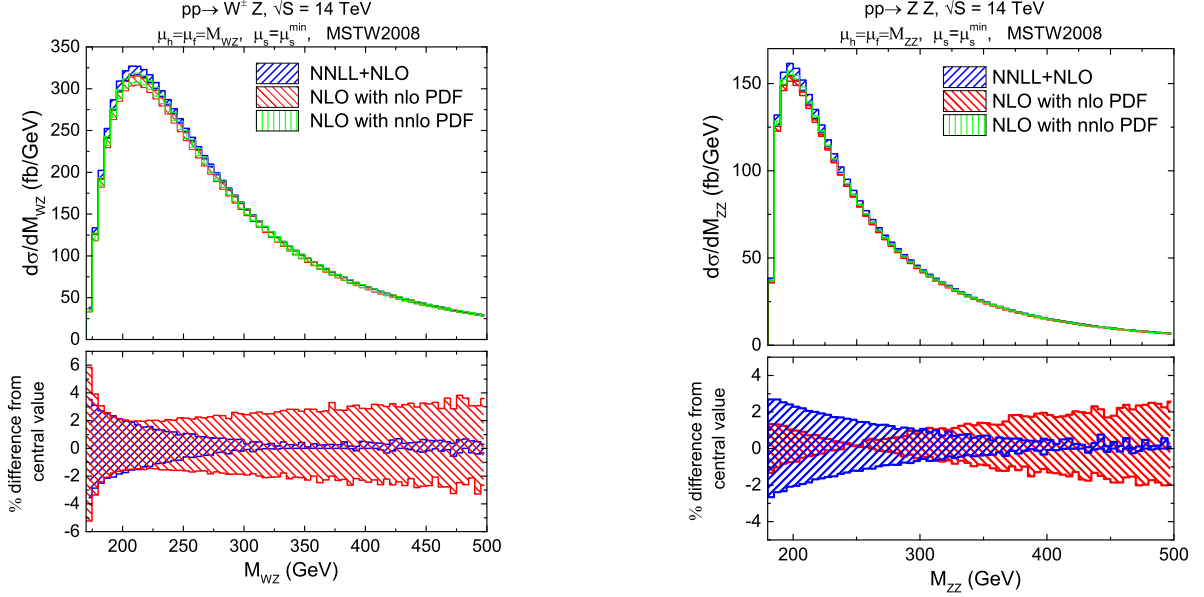


FIG. 4: Comparison of NNLL+NLO resummation results with NLO predictions, and their factorization scale uncertainties from respective central values at $\sqrt{S} = 14$ TeV. The Blue lines are the NNLL+NLO resummation results, the red lines are the NLO prediction with nlo PDF, while the green lines are those with nnlo PDF.

(up). The blue bands correspond to the NNLL+NLO resummation results, and the red bands are the NLO results with nlo PDFs. The NLO predictions with nnlo PDFs are also shown as the green bands. Comparing with the green and the blue bands, we can find that the main corrections come from the resummation effects, but not the PDFs. Fig. 4 (down) are the deviation from the results of the NNLL+NLO resummation and NLO predictions with nlo PDFs at the central scales, respectively. The NLO results with nnlo PDFs are not shown here, because they are almost the same as the results with nlo PDFs. We can see that in the large invariant mass region, the μ_f dependences of the NNLL+NLO resummation results are much smaller than those of the NLO results. Besides, the μ_f dependences of the $W^\pm Z$ production are smaller than that of the ZZ production. Because there are larger scale dependences in the $W^\pm Z$ fixed-order term, which can cancel out more scale dependences in the resummed part as mentioned above, than the case of the ZZ production.

The ratio of the NNLL+NLO prediction, with (without) π^2 enhancements effects, to the NLO results are shown in the Fig. 5. For dash bands, only the regular soft gluon

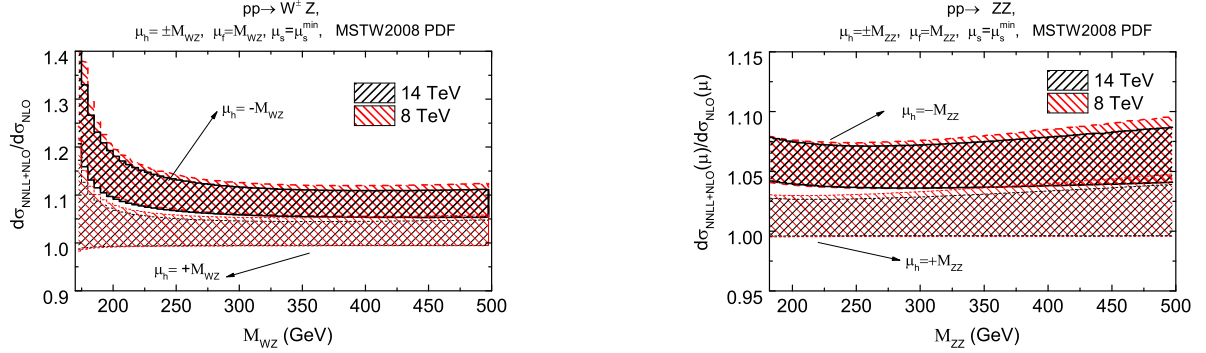


FIG. 5: The ratio of the NNLL+NLO results, with and without the π^2 enhancements effects, to the NLO predictions.

resummation effects are included, while for solid bands the π^2 enhancements effects are also included. For the both cases, in the large invariant mass region, the corrections are stable, and about 9% (2%) for $W^\pm Z$ production and 6% (1%) for ZZ production with (without) the π^2 enhancements effects, respectively. The large corrections in the low invariant mass region are mainly due to the π^2 enhancement effects, especially for $W^\pm Z$ production. The contributions of the π^2 enhancement effects for the gauge boson pair are similar to those found for Drell-Yan process, which are proportional to the $\alpha_s(\mu_h^2)$ at LO [35, 37]. Thus, the corrections become large at small invariant mass. In the following, we will always include the effects of the π^2 resummation.

B. Invariant mass distribution and total cross sections

In Fig. 6, the full invariant mass distribution for $W^\pm Z$ and ZZ production for various energies are shown. We also include contributions from gluon initial states in ZZ productions. The peak position are at about 210 GeV for $W^\pm Z$ production and 200 GeV for ZZ production, respectively. With the increasing of the collider energy, the peak position moves a little to the high invariant mass region.

In Fig. 7, we compare the results of the NNLL+NLO resummation and the POWHEG [38] at $\sqrt{S} = 8$ TeV, where the off-shell effects, the singly resonant contribution and interference with identical fermions are ignored in POWHEG. Both results agree with each other in most regions. The slight differences mainly lie in the peak region.

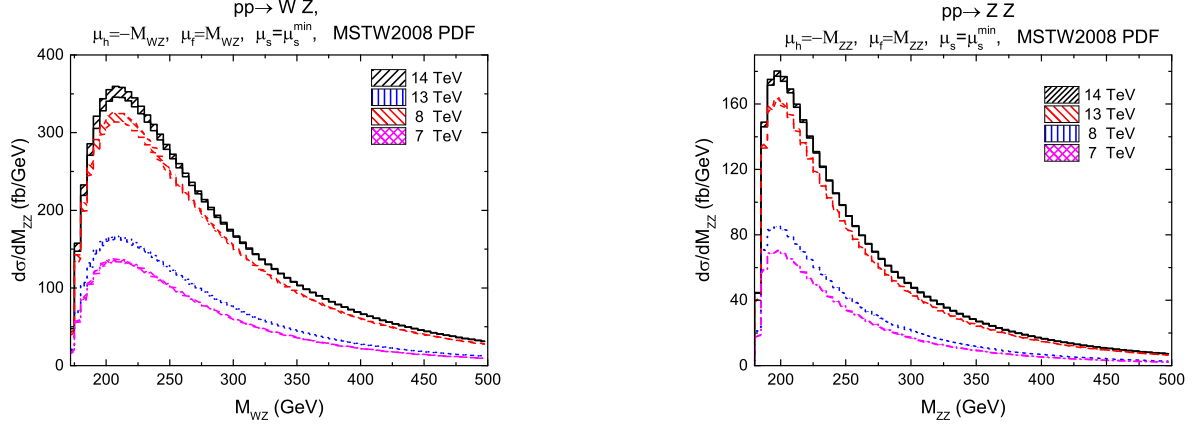


FIG. 6: The invariant mass distributions with $\sqrt{S} = 7, 8, 13$ and 14 TeV, and the scale is $\mu_h^2 = -M_{VZ}^2$ and $\mu_s = \mu_s^{\min}$.

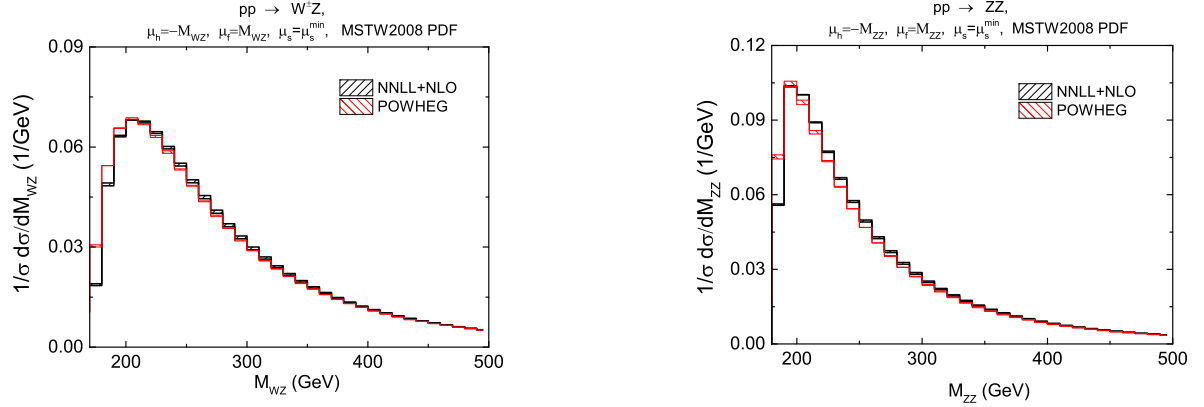


FIG. 7: Comparison of normalized invariant mass distribution for $W^\pm Z$ and ZZ productions between POWHEG and resummation predictions at the LHC with $\sqrt{S} = 8$ TeV.

In Table I, we summarize the total cross sections for $W^\pm Z$ production at the LHC. The first row is the NLO cross sections for $q\bar{q}'$ initial states. The second row is the NNLL+NLO resummation predictions. The third row is the resummation results including the π^2 enhancement effects.

Table II are the results for ZZ production. σ^{gg} are the gg channel contributions, which are calculated with nlo PDFs. And $\sigma_{\text{tot}}^{\text{NNLL+NLO}}$ are the total cross sections of NNLL+NLO resummation, including NLO gg contributions. Comparing with the ZZ production, the π^2 enhancement effects are significant for $W^\pm Z$ production, which come from the differences

of the scale independent term in the hard function between the two channels [17, 22].

In Table I and II, the uncertainties arise from varying the hard, soft scales and the factorization scale each separately by a factor of two around the default choice. These uncertainties are added up in quadrature. The uncertainties of the resummation results increase with the center-of-mass energy. For $W^\pm Z$ production, the uncertainties for $\sigma_{\pi^2}^{\text{NNLL+NLO}}$ are much better than σ^{NLO} in any center-of-mass energy. For ZZ production at $\sqrt{S} = 13$, and 14 TeV, although the factorization scale dependences for $\sigma_{\pi^2}^{\text{NNLL+NLO}}$ are less than those for σ^{NLO} , after taking the soft and hard scale variation into account, the uncertainties become a little greater than that of σ^{NLO} .

σ (pb)	$\sqrt{S} = 7$ TeV	$\sqrt{S} = 8$ TeV	$\sqrt{S} = 13$ TeV	$\sqrt{S} = 14$ TeV
σ^{NLO}	$17.28^{+0.65}_{-0.52}$	$21.37^{+0.76}_{-0.61}$	$44.16^{+1.20}_{-0.94}$	$49.09^{+1.27}_{-0.10}$
$\sigma^{\text{NNLL+NLO}}$	$17.88^{+0.43}_{-0.22}$	$22.10^{+0.53}_{-0.27}$	$45.69^{+1.07}_{-0.58}$	$50.77^{+1.20}_{-0.65}$
$\sigma_{\pi^2}^{\text{NNLL+NLO}}$	$19.40^{+0.30}_{-0.24}$	$23.96^{+0.37}_{-0.30}$	$49.35^{+0.83}_{-0.68}$	$54.81^{+0.94}_{-0.77}$

TABLE I: Total cross sections for $pp \rightarrow W^\pm Z$ with MSTW2008 PDFs.

σ (pb)	$\sqrt{S} = 7$ TeV	$\sqrt{S} = 8$ TeV	$\sqrt{S} = 13$ TeV	$\sqrt{S} = 14$ TeV
σ^{NLO}	$5.86^{+0.10}_{-0.07}$	$7.16^{+0.10}_{-0.07}$	$14.26^{+0.08}_{-0.02}$	$15.77^{+0.07}_{-0.01}$
σ^{gg}	$0.28^{+0.08}_{-0.06}$	$0.38^{+0.1}_{-0.09}$	$1.06^{+0.24}_{-0.20}$	$1.22^{+0.27}_{-0.21}$
$\sigma^{\text{NNLL+NLO}}$	$5.98^{+0.08}_{-0.07}$	$7.33^{+0.10}_{-0.10}$	$14.66^{+0.27}_{-0.24}$	$16.21^{+0.31}_{-0.27}$
$\sigma_{\pi^2}^{\text{NNLL+NLO}}$	$6.25^{+0.04}_{-0.08}$	$7.65^{+0.11}_{-0.11}$	$15.31^{+0.23}_{-0.25}$	$16.94^{+0.27}_{-0.30}$
$\sigma_{\text{tot}}^{\text{NNLL+NLO}}$	$6.53^{+0.09}_{-0.10}$	$8.03^{+0.15}_{-0.14}$	$16.37^{+0.33}_{-0.32}$	$18.16^{+0.38}_{-0.37}$

TABLE II: Total cross sections for $pp \rightarrow ZZ$ with MSTW2008 PDFs.

In Fig. 8, we summarize and compare the total cross section with the LHC experiment data. Obviously, within theoretical and experimental uncertainties, our NNLL+NLO predictions are consistent with the experimental data [15]. The largest deviation is less than 2 σ as compared to ATLAS data at $\sqrt{S} = 8$ TeV.

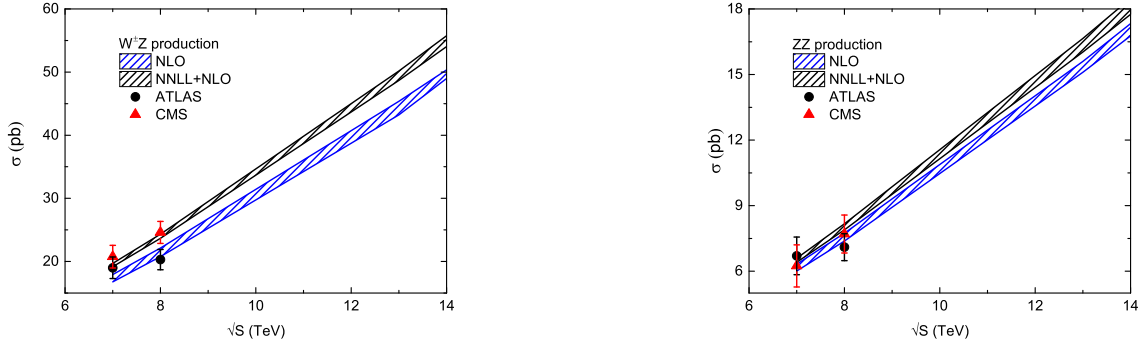


FIG. 8: The total cross sections with different center-of-mass energies for gauge boson pair production at the LHC.

IV. CONCLUSION

We have calculated the threshold resummation for $W^\pm Z$ and ZZ pair productions at the NNLL + NLO accuracy at the LHC with SCET. We present the invariant mass distributions and the total cross sections, including π^2 enhancement effects, which show that the resummation effects increase the NLO total cross section by about 7% for ZZ production and 12% for $W^\pm Z$ production, respectively. Our results also agree well with the experimental data reported by ATLAS and CMS collaboration both at $\sqrt{S} = 7$ TeV and at $\sqrt{S} = 8$ TeV within theoretical and experimental uncertainties.

V. ACKNOWLEDGMENTS

This work is supported in part by the National Natural Science Foundation of China under Grants No. 11375013 and No. 11135003.

-
- [1] T. Aaltonen et al. (CDF Collaboration), Phys.Rev.Lett. **108**, 101801 (2012), 1112.2978.
 - [2] V. M. Abazov et al. (D0 Collaboration), Phys.Rev. **D85**, 112005 (2012), 1201.5652.
 - [3] V. M. Abazov et al. (D0 Collaboration), Phys.Rev. **D88**, 032008 (2013), 1304.5422.
 - [4] G. Aad et al. (ATLAS Collaboration), Phys.Rev.Lett. **108**, 041804 (2012), 1110.5016.
 - [5] G. Aad et al. (ATLAS Collaboration), Eur.Phys.J. **C72**, 2173 (2012), 1208.1390.

- [6] G. Aad et al. (ATLAS Collaboration), Phys.Lett. **B709**, 341 (2012), 1111.5570.
- [7] Tech. Rep. ATLAS-CONF-2014-015, CERN (2014).
- [8] Tech. Rep. ATLAS-CONF-2013-021, CERN (2013).
- [9] Tech. Rep. ATLAS-CONF-2013-020, CERN (2013).
- [10] S. Chatrchyan et al. (CMS Collaboration), JHEP **1301**, 063 (2013), 1211.4890.
- [11] Tech. Rep. CMS-PAS-SMP-12-016, CERN (2013).
- [12] Tech. Rep. CMS-PAS-SMP-13-005, CERN (2013).
- [13] Tech. Rep. CMS-PAS-SMP-13-011, CERN (2013).
- [14] S. Chatrchyan et al. (CMS Collaboration) (2014), 1403.3047.
- [15] J. Wang (ATLAS Collaboration, D0 Collaboration, CMS Collaboration) (2014), 1403.1415.
- [16] J. Ohnemus and J. F. Owens, Phys. Rev. D **43**, 3626 (1991).
- [17] B. Mele, P. Nason, and G. Ridolfi, Nucl.Phys. **B357**, 409 (1991).
- [18] J. Ohnemus, Phys. Rev. D **50**, 1931 (1994).
- [19] L. Dixon, Z. Kunszt, and A. Signer, Phys. Rev. D **60**, 114037 (1999).
- [20] J. M. Campbell and R. K. Ellis, Phys. Rev. D **60**, 113006 (1999).
- [21] L. Dixon, Z. Kunszt, and A. Signer, Nuclear Physics B **531**, 3 (1998), ISSN 0550-3213.
- [22] S. Frixione, P. Nason, and G. Ridolfi, Nucl.Phys. **B383**, 3 (1992).
- [23] Y. Wang, C. S. Li, Z. L. Liu, D. Y. Shao, and H. T. Li, Phys.Rev. **D88**, 114017 (2013), 1307.7520.
- [24] F. Campanario and S. Sapeta, Phys.Lett. **B718**, 100 (2012), 1209.4595.
- [25] F. Cascioli, T. Gehrmann, M. Grazzini, S. Kallweit, P. Maierhofer, et al. (2014), 1405.2219.
- [26] T. Gehrmann, L. Tancredi, and E. Weihs, JHEP **1308**, 070 (2013), 1306.6344.
- [27] J. M. Henn, K. Melnikov, and V. A. Smirnov (2014), 1402.7078.
- [28] T. Gehrmann, A. von Manteuffel, L. Tancredi, and E. Weihs (2014), 1404.4853.
- [29] F. Caola, J. M. Henn, K. Melnikov, and V. A. Smirnov (2014), 1404.5590.
- [30] S. Dawson, I. M. Lewis, and M. Zeng, Phys. Rev. D **88**, 054028 (2013), URL <http://link.aps.org/doi/10.1103/PhysRevD.88.054028>.
- [31] M. Beneke, A. Chapovsky, M. Diehl, and T. Feldmann, Nucl.Phys. **B643**, 431 (2002), hep-ph/0206152.
- [32] C. W. Bauer, S. Fleming, D. Pirjol, and I. W. Stewart, Phys.Rev. **D63**, 114020 (2001), hep-ph/0011336.

- [33] C. W. Bauer, D. Pirjol, and I. W. Stewart, Phys.Rev. **D65**, 054022 (2002), hep-ph/0109045.
- [34] T. Becher, M. Neubert, and G. Xu, JHEP **0807**, 030 (2008), 0710.0680.
- [35] V. Ahrens, T. Becher, M. Neubert, and L. L. Yang, Phys.Rev. **D79**, 033013 (2009), 0808.3008.
- [36] J. Beringer et al. (Particle Data Group), Phys.Rev. **D86**, 010001 (2012).
- [37] D. Y. Shao, C. S. Li, H. T. Li, and J. Wang, JHEP **1307**, 169 (2013), 1301.1245.
- [38] P. Nason and G. Zanderighi (2013), 1311.1365.